Journal of Catalysis **188,** 83–89 (1999)
Article ID jcat.1999.2628, available online at http://www.idealibrary.com on IDEAL®

Ammonia Synthesis over a Multipromoted Iron Catalyst: Extended Set of Activity Measurements, Microkinetic Model, and Hydrogen Inhibition

Jens Sehested,*,[1] Claus J. H. Jacobsen,* Eric Törnqvist,* Said Rokni,* and Per Stoltze†

*Haldor Topsøe Research Laboratories, Nymøllevej 55, DK-2800 Lyngby, Denmark; and †Center for Atomic-scale Materials Physics (CAMP), Department of Physics, Building 307, Technical University of Denmark, DK-2800 Lyngby, Denmark

Received March 1, 1999; revised May 12, 1999; accepted June 30, 1999

The ammonia synthesis activity of a multipromoted iron catalyst (KM1R, Haldor Topsøe A/S) is reported for a wide range of conditions. The $H_2:N_2$ ratio is varied by a factor of 10, the total pressures are between 1 and 100 bar, and temperatures are in the range 320–440°C. Data obtained here and literature data are compared. It is concluded that water poisoning is negligible in the present activity measurements and that hydrogen inhibition is important at the combined conditions of low temperature, low ammonia partial pressure, and high total pressure. From a fit to the activity data a microkinetic model is obtained, which has H^* and N^* as surface species. The equilibrium constant of hydrogen adsorption obtained from single crystal studies, $2.16 \cdot 10^3$ bar$^{0.5}$ exp(-48 kJ mol^{-1} R^{-1} T^{-1}), is used as input for the model. The obtained model parameters are the rate constant at zero coverage, 7.79 mmol g^{-1} s^{-1} bar^{-1} exp(-6.6 kJ mol^{-1} R^{-1} T^{-1}) and the equilibrium constant for the equilibrium between ammonia, hydrogen, and adsorbed nitrogen, 0.027 bar$^{-0.5}$ exp(-27.1 kJ mol^{-1} R^{-1} T^{-1}). From these two parameters a rate of 1.43×10^{12} s^{-1} exp(-162.4 kJ mol^{-1} R^{-1} T^{-1}) for nitrogen desorption is inferred. The performance of the model is compared to three microkinetic models found in the literature. The model gives a quantitative account of the catalytic activity at all the measured degrees of conversions, pressures, and temperatures and is consistent with surface science data.

Key Words: **ammonia synthesis; microkinetic analysis; multipromoted iron catalyst.**

INTRODUCTION

In the literature there are numerous reports of studies of ammonia synthesis over multipromoted iron catalysts, e.g., by Temkin *et al.* (1), Nielsen (2), and Kowalczyk *et al.* (3, 4). However, in most reported experiments, $H_2:N_2$ ratios of 3 : 1 were used. To establish the activity of a multipromoted iron catalyst at different $H_2:N_2$ ratios we measured the activity of the KM1R catalyst (Haldor Topsøe A/S) with the $H_2:N_2$ ratio varied by a factor of 10, the total pressure in the range 1–100 bar, and with temperatures ranging from 320 to 440°C. This extended data set was used to evaluate the microkinetic model also reported here. The catalyst activity was independent of the ammonia partial pressure at the combined conditions of low temperatures, low conversions, and high total pressures. The reason for this unexpected behaviour was investigated in more detail.

Microkinetic models for ammonia synthesis over promoted iron catalysts have been developed from surface science data by Stoltze and Nørskov (5–9), Model I and by Bowker *et al.* (10–13), Model II. Fastrup (14) developed a model from temperature programmed adsorption and desorption (TPA and TPD), as well as chemisorption experiments, Model III. The model of Stoltze and Nørskov included the following reaction steps:

$$N_2(g) + {}^* \rightleftarrows N_2^* \qquad [1, -1]$$

$$N_2^* + {}^* \rightleftarrows 2N^* \qquad [2, -2]$$

$$N^* + H^* \rightleftarrows NH^* + {}^* \qquad [3, -3]$$

$$NH^* + H^* \rightleftarrows NH_2^* + {}^* \qquad [4, -4]$$

$$NH_2^* + H^* \rightleftarrows NH_3^* + {}^* \qquad [5, -5]$$

$$NH_3^* \rightleftarrows NH_3(g) + {}^* \qquad [6, -6]$$

$$H_2(g) + 2^* \rightleftarrows 2H^* \qquad [7, -7]$$

where * and X^* denote a free site and a species X bonded to the surface, respectively. All steps except [2] were assumed to be in equilibrium and reaction [2] the rate determining step. Stoltze and Nørskov used statistical mechanics to describe the reactions in their model. Dumesic and Treviño (15) derived the Arrhenius form of the model at 450°C and this formulation will be used in the following study. The reaction schemes of the microkinetic models by Bowker *et al.* (10–13) and by Fastrup (14) are very similar to the scheme above. Bowker *et al.* divided step (7) into two, where molecular hydrogen adsorbs before dissociation, while Fastrup combined steps [1] and [2] into one step. These changes do not influence the overall kinetics since N_2^* and H_2^* are both in equilibrium with N_2 and H_2, respectively, and have negligible coverages.

[1] To whom correspondence should be addressed. E-mail: JSS@topsoe.dk; Fax: +45 45272999.

0021-9517/99 $30.00

Ammonia synthesis activities generated by Models I–III have all been reported (5, 14–16) to almost quantitatively predict the activity of a commercial iron-based catalyst even though the models contain significant differences in activation and binding energies. For example, the activation energy for steps (1) and (2) combined was approximately −14.6, −14.7, and 57.6 kJ/mol for Models I, II, and III, respectively. Another example is the enthalpy of desorption of N_2, where Models I, II, and III use 169.6, 213.7, and 88.7 kJ/mol, respectively.

In the present work a microkinetic model is developed where the key parameters are obtained from a fit to catalytic activity data published recently (3), Model IV. The performance of all microkinetic models are tested using the activity measurements of Nielsen (2) and finally, the results of Model IV are compared to the extended set of activity data obtained in this work.

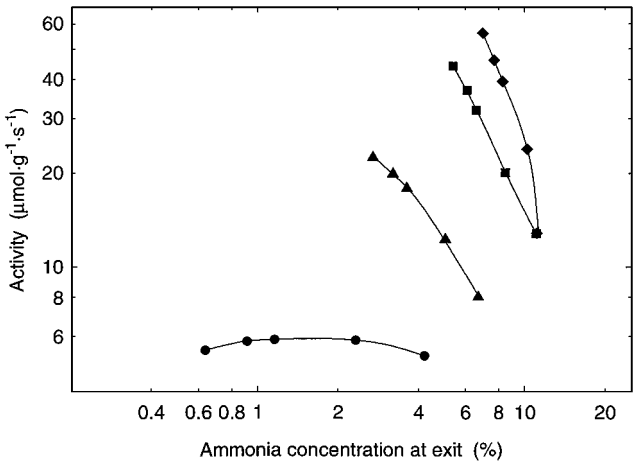

FIG. 1. Activity of KM1R measured at 320, 360, 400, and 440°C plotted as circles, triangles, squares, and diamonds, respectively. 0.203 g catalyst, 100 bar total pressure, $H_2 : N_2 = 3 : 1$, 40–267 ml/min total flow at STP was used.

METHODS

The experimental setup for activity measurements used in this work consists of a glass-lined stainless steel microreactor (i.d. = 4 mm) loaded with 0.2 g of KM1R ammonia synthesis catalyst with particle size of 0.3–0.8 mm. It was checked by measurement of catalyst particles of 0.2–0.4 mm that the activity is not influenced by particle size effects. KM1R is a triply promoted iron catalyst containing ca. 2.8% CaO, 0.60% K_2O, 2.5% Al_2O_3, and 94% Fe. It is prepared by fusion of the constituent oxides followed by cooling to room temperature. The reduction process has been described together with a detailed characterisation by Nielsen (2). The catalyst size was 1.5–3 mm under reduction. Reduction of this size range gives rise to a 10% reduction in activity compared to reduction of infinitely small particles (2). Total pressures in the range of 1–100 bar, temperatures between 320 and 440°C, and feed flows of 40 to 400 ml/min (STP) are used. The flow of each gas line is controlled by an electronic mass flow controller. All gasses used were of 99.9999% purity and were further purified by flowing them over a large volume of activated KM1R catalyst kept at room temperature. These catalysts were reactivated monthly. Possible oxygen poisoning of the catalyst was checked as described below. Ammonia concentrations were measured by two nondispersive infrared detectors (BINOS, Leybold-Heraus) working in different concentration ranges which were calibrated weekly by reference gasses.

RESULTS

The full set of activity data is not given here due to space limitations; however, it can be obtained directly from the authors. The activity of the catalyst at 100 bar total pressure, $H_2 : N_2 = 3 : 1$, and the temperatures of 320, 360, 400, and 440°C is shown in Fig. 1. The data obtained at 100 bar total pressure and 400°C were compared to the data from Nielsen (2). The activity of the catalyst of Nielsen is 15% lower than the catalyst used here, which could be explained by higher gas purity in the more recent experiments and by optimisation of the KM1R catalyst.

Interestingly, no ammonia inhibition is seen at 320°C which could indicate water poisoning of the catalyst since oxygen poisoning is expected to reduce the ammonia inhibition of the catalyst (5). To test for oxygen poisoning the procedure of Fastrup and Nielsen (17) was used. The activity of the catalyst was measured at 400°C after which the temperature was rapidly reduced to 300°C and the activity was monitored for 45 h. Any significant oxygen poisoning would result in a decrease in the activity during this period. Fastrup and Nielsen recommended 1 bar total pressure for these experiments to reduce the time for the change in temperature and stabilisation of the ammonia concentration. However, since the lack of ammonia inhibition was only observed at 100 bar total pressure and the time for the temperature drop at this pressure was reasonable, approximately 30 min, the pressure was not reduced to one bar. The ammonia concentration at the outlet of the reactor after the change in temperature showed no significant drop (approximately 6.5% in 2 days) during the 45 h of measurements. Theoretically (5) and experimentally (17, 18) it has been shown that at 300°C, oxygen from water and other oxygen containing compounds bind strongly to the surface and cannot be removed. The catalyst surface can at maximum contain 25 μmol O*/g KM1R catalyst (18). With the catalyst loading of 0.2 g of KM1R, 5 μmol of oxygen can be present on the surface. The flow rate used for the data was 267 ml/min (STP). The catalyst looses approximately 6.5% of its activity in two days. To cover 6.5% of the surface with

oxygen in two days with a flow of 267 ml/min, the content of water in the feed is necessarily less than 0.01 ppm. Alternatively, the catalyst could have been water poisoned during the temperature drop, implying that the observed activity is that of an oxygen poisoned catalyst. The water concentration would have to be approximately 14 ppm to poison the catalyst in half an hour, which is far higher than in the feed before purification. In addition, the activity at 300°C is far higher than expected for a poisoned catalyst (19). As a final check the temperature was increased to 400°C after the 45 h at 300°C and the activity returned to the same value as previously. Therefore, we conclude that there was no oxygen poisoning of the catalyst during the experiments of this report. However, when performing experiments at low temperatures over longer periods (weeks) one should be aware of the risk of oxygen poisoning of the catalyst. Even minimum concentrations of oxygen containing compounds in the feed will eventually deactivate the catalyst.

Since the absence of ammonia inhibition at 320°C and 100 bar total pressure cannot be explained by adsorbed oxygen, one would assume that another species is blocking the surface. Any nitrogen containing species apart from N_2^* can be ruled out since they all will lead to ammonia inhibition (5). Based on surface science (20) and catalyst studies (21) the concentration of N_2^* on the catalyst surface is negligible. Hence, the species is presumably H^*. To further investigate this possibility, experiments were performed at 100 bar total pressure, an initial $H_2:N_2$ ratio of 3 : 1, and at temperatures of 320, 360, and 400°C. After recording the activity at the ratio $H_2:N_2 = 3:1$, part of the hydrogen was substituted by helium. Figure 2 displays the ammonia concentration at the reactor exit as a function of the hydrogen pressure. At 360 and 400°C the behaviour is as expected. A decrease in the ammonia concentration is observed when the hydrogen partial pressure is lowered. However, at 320°C an increase in the ammonia concentration is seen as the hydrogen pressure is decreased, with a slope of approximately −1.3. This is the reaction order in hydrogen, and it is close to −1, which is predicted by the microkinetic models if hydrogen is completely covering the surface.

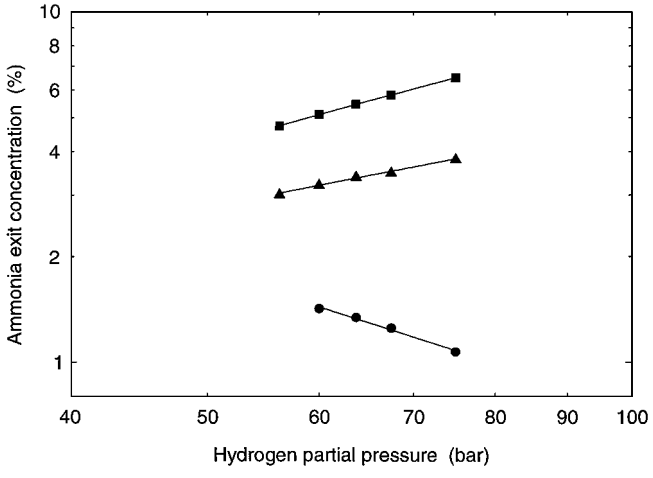

FIG. 2. Ammonia concentration as a function of hydrogen partial pressure at 320°C (circles), 360°C (triangles), and 400°C (squares). Power law lines are given to aid the visual inspection of the data.

There are two additional pieces of experimental evidence that support the conclusion about hydrogen inhibition. First, in our data set the ammonia inhibition increases as the total pressure and the $H_2:N_2$ ratio decrease. Second, it was reported by Nielsen (22) that the ammonia synthesis rates fall faster for $H_2:N_2 = 3:1$ than for $H_2:N_2 = 1:1$ when reducing the temperatures from 420 to 300°C. Both observations can be explained by the equilibrium $N^* + 2H_2 \rightleftarrows NH_3 + H^*$. An increase in the hydrogen partial pressure at a given ammonia concentration will "push" the most abundant nitrogen containing surface species, N^*, off the catalyst. In addition, a decrease in the temperature "pushes" the equilibrium towards the right.

DISCUSSION

This section consists of three parts. First, a microkinetic model is developed from a fit to activity data and the key parameters are discussed. Then the results from the microkinetic Models I, II, III, and IV are compared to the data of Nielsen (2). Finally, the results of Model IV are compared to the new data set of the present report.

To identify and derive the relevant parameters of a microkinetic model from activity data, it is necessary to have data which cover a wide range of ammonia partial pressures. Preferably, the catalyst activity should be given as the differential activity, which is obtained from a CSTR reactor. Therefore, we used the results reported by Kowalczyk (3) who studied a triple promoted iron catalyst with an ammonia synthesis activity similar to our KM1R catalyst. The activities were measured at 100 bar total pressure with an $H_2:N_2$ ratio of 3 : 1 and at temperatures of 370, 400, 430, and 470°C. The results are displayed in Fig. 3.

As a first assumption to fit the data, hydrogen (H^*) and nitrogen (N^*) are assumed to be the only species present in appreciable amounts at the catalyst surface. The model of Stoltze and Nørskov (5–8) predicts approximately 15% coverage of NH^* on the surface at 400°C, 100 bar total pressure, and with the $H_2:N_2$ ratio of 3 : 1. However, the amount of NH^* is uncertain due to uncertainty in the binding energy of NH^*. The assumption that no NH^* is on the surface if, in fact, 15% is present will to a first approximation be a 20% increase of the equilibrium constant for the equilibrium between nitrogen on the surface and ammonia and hydrogen in the gas phase (K_a, see below), as well as an increase in the hydrogen reaction order of approximately 5%. Hence, with our present understanding of the ammonia synthesis the first assumption seems to be reasonable in order to reduce the number of fitting parameters. Using

this assumption and the approach of Stoltze and Nørskov (5–9) the ammonia synthesis reaction rate, r, is then

$$r = 2N_S K_1 k_2 \theta_*^2 \left(P_{N_2} - \frac{P_{NH_3}^2}{P_{H_2}^3 K_{eq}} \right)$$
$$= 2N_S K_1 k_2 \left(P_{N_2} - \frac{P_{NH_3}^2}{P_{H_2}^3 K_{eq}} \right) \left(1 + \frac{P_{NH_3}}{P_{H_2}^{1.5} K_a} + \frac{P_{H_2}^{0.5}}{K_b} \right)^{-2},$$

where K_1 is the equilibrium constant for reaction [1], k_2 is the rate constant for reaction [2], K_{eq} is the equilibrium constant for the overall reaction, N_S is the total number of active sites per gram, θ_*, θ_{N^*}, θ_{H^*} are the fraction of free sites, fraction of N*, and fraction of H* on the catalyst surface, respectively, and K_a and K_b are equilibrium constants for the reactions given below. Note that these equilibrium constants are not dimensionless.

$$N_2 + {}^* \rightleftarrows N_2^*, k_1, k_{-1}$$
$$N_2^* + {}^* \rightleftarrows 2N^*, k_2, k_{-2}$$
$$N^* + 3/2H_2 \rightleftarrows NH_3 + {}^*, K_a = \frac{P_{NH_3}\theta_*}{P_{H_2}^{1.5}\theta_{N^*}}$$
$$H^* \rightleftarrows 1/2H_2 + {}^*, K_b = \frac{P_{H_2}^{0.5}\theta_*}{\theta_{H^*}}$$

We are now left with three parameters, $2N_S K_1 k_2$, K_a, and K_b. Only two parameters can be derived from the data in Fig. 3; hence we have to make another assumption. We have chosen to set K_b equal to the equilibrium constant derived by Dumesic and Trevino (15) from the model of Stoltze and Nørskov (5–9) but substituting their binding energy with the binding energy derived for potassium promoted Fe(111) at low coverage (23), $K_b = 2.16 \times 10^3$ bar$^{0.5}$ exp(−48 kJ mol^{-1} R^{-1} T^{-1}). A support for this choice, one may argue, is that single crystal experiments give a measure of the H* binding energy to what is believed to be the active site. Furthermore, hydrogen adsorbed at potassium promoted Fe(100) has approximately the same binding energy as at potassium promoted Fe(111) (23). So, in the event that Fe(100) would in fact be the most active surface face, the error in binding energy of hydrogen would not be large. An alternative method of obtaining K_b would be from hydrogen chemisorption experiments of the catalyst, where all absorption sites contribute to the hydrogen adsorption. However, it might be difficult to decide whether strongly or weakly bonded hydrogen or all hydrogen is bonded to active sites. In addition, with our choice of K_b we may obtain a microkinetic model which is consistent with surface science data.

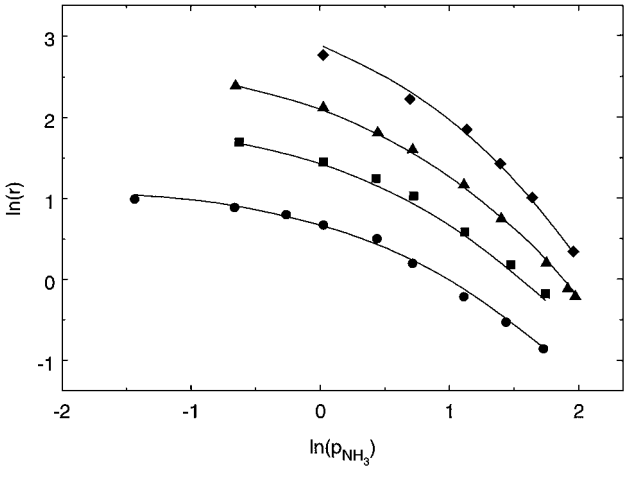

FIG. 3. The activities obtained by Kowalczyk (3) for a triple promoted iron catalyst at 100 bar total pressures using $H_2:N_2 = 3:1$ and temperatures of 370, 400, 430, and 470°C. The smooth lines are a fit to the data. See text for details.

It is appropriate to note that if it is assumed that the equilibrium constant for reaction [7] derived by Fastrup (14) is used instead, we still get a satisfactory fit to the data of Fig. 3. However, there will be a difference in the predicted coverages of hydrogen and nitrogen especially at low pressures and therefore the results of the models are compared to the experimental data carried out at 1 bar. The model with our choice of K_b gives a slightly better description of the data (30% lower standard deviation) than with the value of K_b derived by Fastrup (14). However, clearly more work is needed to effectively discriminate between the two different approaches.

Using $K_b = 2.16 \times 10^3$ bar$^{0.5}$ exp(−48 kJ mol^{-1} R^{-1} T^{-1}), the natural logarithm of the rate is given by

$$\ln(r) = \ln(N_S K_1 k_2) + \ln\left(P_{N_2} - \frac{P_{NH_3}^2}{P_{H_2}^3 K_{eq}} \right) - 2\ln\left(1 + \frac{P_{NH_3}}{P_{H_2}^{1.5} K_a} + \frac{P_{H_2}^{0.5}}{K_b} \right)$$

The temperature dependence of the two parameters $\ln(2N_S K_1 k_2)$ and $\ln(K_a)$ are accounted for as follows: $\ln(2N_S K_1 k_2 K_b^2) = a - bT^{-1}$ and $\ln(K_b/K_a) = c - dT^{-1}$. The nonlinear least squares fit of the expression above varying a, b, c, and d are displayed in Fig. 3 and it is clear that the model gives an excellent fit to the activity data. The obtained parameters are: $\ln(2N_S K_1 k_2) = 9.0 \pm 1.1 - (800 \pm 700\ \text{K})\ T^{-1}$ and $\ln(K_a) = -3.6 \pm 1.0 - (3300 \pm 700\ \text{K})\ T^{-1}$ where $N_S 2K_1 k_2$ are given in μmol g^{-1} s^{-1} bar^{-1} and K_a in bar$^{-0.5}$. Using $K_{eq} \approx -26.900 + 12200\ T^{-1}$ we obtain $\ln(2N_S k_{-2}) = 28.7 \pm 2.3 - (19500 \pm 1500\ \text{K})\ T^{-1}$ if the uncertainty on the equilibrium constant is assumed to be negligible. In nonlogarithmic form the parameters derived above are calculated to be: $2N_S K_1 k_2 = 7790$ μmol g^{-1} s^{-1} bar^{-1} exp(−6.6 kJ mol^{-1} R^{-1} T^{-1}), $K_a = 0.027$ bar$^{-0.5}$ exp(−27.1 kJ mol^{-1} R^{-1} T^{-1}), $K_{eq} = 2.03 \times 10^{-12}$ bar^{-2}

TABLE 1

Comparison between the Parameters of the Three Previously Proposed Microkinetic Models and the Model Derived Here (Model IV)

	K_a ($bar^{-0.5}$)	$2K_1k_2$ ($bar^{-1}\,s^{-1}$)	$2k_{-2}$ (s^{-1})
Model I[a]	$5.15\times10^{-3}\exp(-31.7\ kJ\,mol^{-1}\,R^{-1}\,T^{-1})$	$116\exp(14.6\ kJ\,mol^{-1}\,R^{-1}\,T^{-1})$	$2.64\times10^{9}\exp(-155.0\ kJ\,mol^{-1}\,R^{-1}\,T^{-1})$
Model II	$5.54\times10^{-2}\exp(-53.0\ kJ\,mol^{-1}\,R^{-1}\,T^{-1})$	$974\exp(14.7\ kJ\,mol^{-1}\,R^{-1}\,T^{-1})$	$5.26\times10^{12}\exp(-199.0\ kJ\,mol^{-1}\,R^{-1}\,T^{-1})$
Model III	$2.76\times10^{-4}\exp(9.0\ kJ\,mol^{-1}\,R^{-1}\,T^{-1})$	$4.0\times10^{4}\exp(-57.6\ kJ\,mol^{-1}\,R^{-1}\,T^{-1})$	$2.6\times10^{9}\exp(-146.3\ kJ\,mol^{-1}\,R^{-1}\,T^{-1})$
Model IV[b]	$2.73\times10^{-2}\exp(-27.1\ kJ\,mol^{-1}\,R^{-1}\,T^{-1})$	$150\exp(-6.6\ kJ\,mol^{-1}\,R^{-1}\,T^{-1})$	$5.51\times10^{10}\exp(-162.4\ kJ\,mol^{-1}\,R^{-1}\,T^{-1})$

[a] Model built on statistical mechanics. The preexponential factors and activation energies were therefore derived at a temperature of 450°C (15).
[b] Assuming an active site density of 52 μmol g^{-1}.

$\exp(101.6\ kJ\,mol^{-1}\,R^{-1}\,T^{-1})$, and $2N_Sk_{-2} = 2.87\times10^{12}\ \mu mol\ g^{-1}\,s^{-1}\exp(-162.4\ kJ\,mol^{-1}\,R^{-1}\,T^{-1})$.

These values can be compared to the values of K_a, $2K_1k_2$, and $2k_{-2}$ used in Models I–III if the number of active sites is known. From the nitrogen desorption studies reported by Fastrup (14) and Muhler *et al.* (18) it is possible to get an estimate of this number, and Fastrup reports 52 μmol g^{-1} for the first peak in a desorption experiment. Using this value we obtain $k_{-2} = 2.76\times10^{10}\ s^{-1}\exp(-162.4\ kJ\,mol^{-1}\,R^{-1}\,T^{-1})$ and desorption rates which are similar to those estimated by Muhler *et al.* and Fastrup even though these authors have significantly lower binding energies and preexponential factors. However, the activation energy of 162.4 kJ mol^{-1} is in excellent agreement with the activation energy of 167 kJ mol^{-1} derived from ammonia decomposition over a triple promoted iron catalyst (4).

The values for K_a, $2K_1k_2$, and $2k_{-2}$ are given in Table 1. One of the main differences between the models is the enthalpy of nitrogen chemisorption. The model of Stoltze and Nørskov, Model I, gives $\Delta H(N^*) = 84.8$ kJ/mol at 450°C while Models II and III use an enthalpy of nitrogen chemisorption of 106.9 and 44.4 kJ/mol, respectively. We derive $\Delta H(N^*) = 77.9$ kJ/mol, which is close to the value determined by Stoltze and Nørskov from single crystal studies of pure Fe(111). However, the enthalpy of chemisorption of nitrogen may be different at a pure and a promoted surface.

Our value of $\Delta H(N^*)$ is quite different from the one used in model III, which was derived from TPD and TPA studies of the catalyst. The value of k_{-2} which we derive here reproduces the TPD experiments of both Fastrup (14) and Muhler *et al.* (18), while the TPA experiments of Ref. (14) are not consistent with the current model. At present the reason for this is unknown. However, it is interesting to note that modelling the TPA experiments by use of Models I and IV suggests that a high N^* coverage is found at the catalyst surface already below room temperature. If this is correct it would explain the similarity of the TPA results for singly, doubly, and multipromoted iron catalysts.

Differences between the models also exist in the activation energy of nitrogen dissociation. Models I and II use essentially the same activation energy −14.6 and −14.7 kJ/mol, Model III uses 57.6 kJ/mol, and Model IV uses 6.6 kJ/mol. The difference of about 20 kJ/mol between the activation energy for Models IV and I may be due to uncertainty in the single crystal data of Model I and the activation energy determined for Model IV. The difference of 50–70 kJ/mol between Model III and the other models is beyond any experimental uncertainty.

Generally, the parameters for Models I and IV are similar. This is perhaps not too surprising since both models give a good description of the catalyst activity and have the same equilibrium constant for hydrogen dissociation. However, it underlines the notion that it is possible to predict the activity of a multipromoted iron ammonia catalyst by a model that is consistent with surface science data.

In Fig. 4 the results of the kinetic models are compared to the experimental data by Nielsen (2). It is interesting to note that all models give a relatively good description of the synthesis rate even though the input parameters are very different as shown above. Clearly, for models with a high nitrogen binding energy, it is necessary to use a low or negative activation energy for reaction [2], and for models with high activation energy for reaction [2] it is necessary to use a low nitrogen binding energy to reproduce the activity of the catalyst.

The model developed here and Model III give very similar and quantitative predictions for the high pressure data and the best overall description of the data of the four models. The relative deviation of the predicted values from the experimental values are slightly higher for Model IV than for Model III. However, if the possibly water poisoned low temperature point (331°C) is excluded, the predictions of Model IV are slightly better than those of Model III.

Model IV offers three advantages over Model III. First, the parameters in Model IV are close to the ones derived from surface science experiments. In addition, Model IV is derived from activity data which give the reactivity and reactivity trends of the active phase whereas Model III is derived from TPD, TPA, and chemisorption data where all iron facets and all adsorption sites may contribute. Finally, Model IV gives the best description of the experimental data of the present work. Especially, the trends of the ln(rate) versus $\ln(p_{NH_3})$ plots at low total pressure. However, Model III is predicting the data well and to effectively

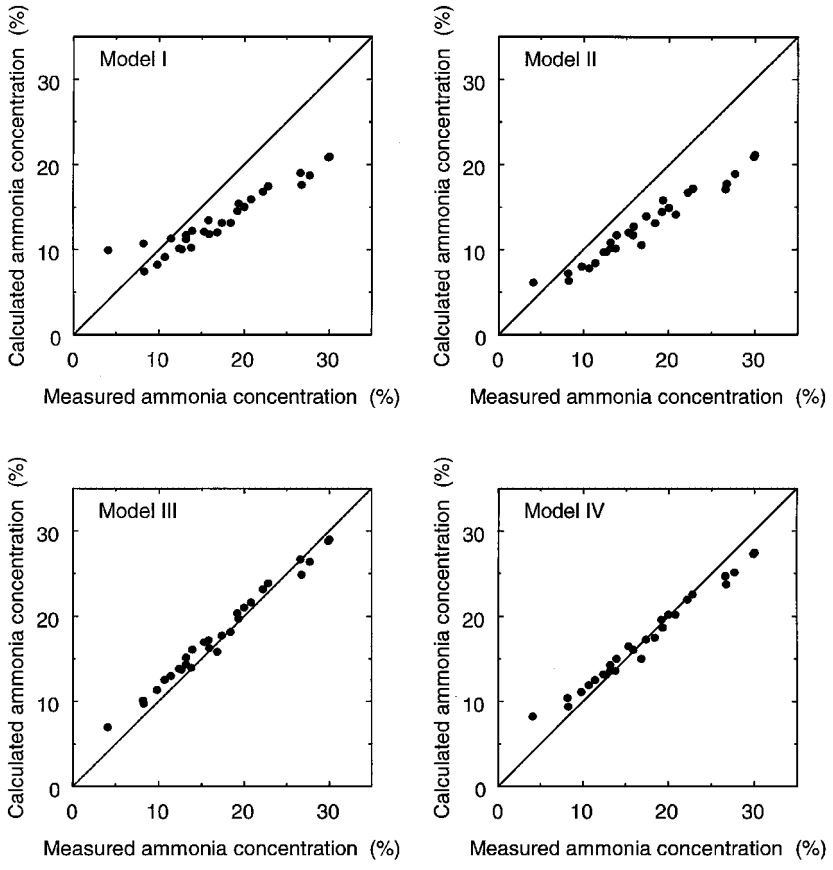

FIG. 4. Ammonia concentration predicted by models I, II, II, and IV plotted as a function of the ammonia concentration measured by Nielsen (2).

discriminate between Models III and IV experiments are needed where the coverages of N^* and H^* are determined at conditions where the models predict very different results, e.g., at low total pressures.

Figure 5 displays the predicted ammonia concentration of model IV versus the measured partial pressures of ammonia. It is clear that the model gives a quantitative description of the data. The relative standard deviation of the ammonia percent predicted by Model IV is 18%. Of course, important assumptions have been made on the choice of the equilibrium constant of hydrogen adsorption, the sole presence of N^* and H^* at the surface, the notion that the adsorption follows Langmuir isotherms, and that adsorption is competitive. These assumptions may not be strictly valid. However, the good reproduction of the experimental data suggests that the assumptions are reasonable and that the basic principles of the model are correct.

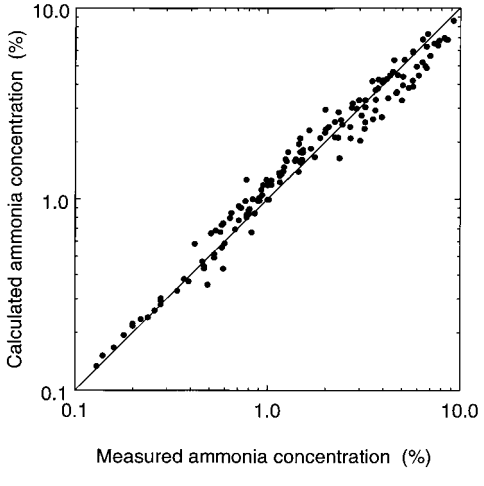

FIG. 5. Ammonia concentration predicted by Model IV plotted as a function of the ammonia concentration measured in the present work.

CONCLUSION

The activity of a multipromoted iron catalyst is measured at total pressures of 1 to 100 bar, temperatures in the range 320–440°C, and with the hydrogen to nitrogen ratio varied by a factor of 10. The measurements show that at low temperatures and low ammonia pressures, the multipromoted iron catalyst is inhibited by hydrogen. Experiments are conducted to check for possible water poisoning according to the method of Fastrup and Nielsen (17) and it is found that water poisoning of the catalyst is negligible.

A quantitative microkinetic model of a multipromoted iron catalyst is presented which contains parameters that

are close to those derived from surface science experiments and based on Langmuiran adsorption. The model which contains N^* and H^* as the sole surface species and nitrogen dissociation as the rate determining step is obtained from a fit of the differential activity measurements of a multipromoted iron catalyst published by Kowalczyk (3). The equilibrium constant for hydrogen adsorption is taken from single crystal studies of hydrogen on potassium promoted Fe(111). The predictions of the model are compared to the activity measurements of Nielsen (2) and activity data obtained in this work.

The following parameters in the model are determined in this work: $2N_S K_1 k_2 = 7790\ \mu\text{mol g}^{-1}\text{s}^{-1}\text{bar}^{-1}\exp(-6.6\ \text{kJ mol}^{-1}\text{R}^{-1}\text{T}^{-1})$, $K_a = 0.027\ \text{bar}^{-0.5}\ \exp(-27.1\ \text{kJ mol}^{-1}\text{R}^{-1}\text{T}^{-1})$, and $2N_S k_{-2} = 2.86 \times 10^{12}\ \mu\text{mol g}^{-1}\text{s}^{-1}\exp(-162.4\ \text{kJ mol}^{-1}\text{R}^{-1}\text{T}^{-1})$. They are similar to the parameters derived by Stoltze and Nørskov (5–9) from single crystal studies but increase the precision of the model predictions for the commercial iron catalyst.

By using the equilibrium constant for hydrogen adsorption derived by Fastrup (14) from TPD, TPA, and chemisorption experiments of the catalyst, we still obtain a reasonable fit of the activity data at 100 bar total pressure. However, Fastrup's parameters are significantly different from ours and inconsistent with those of surface science studies, e.g., high activation energy for nitrogen dissociation and low nitrogen binding energy.

REFERENCES

1. Temkin, M. I., Morozov, N. M., and Shapatina, E. N., *Kinet. I Kataliz.* **4**, 260 (1963).
2. Nielsen, A., "An Investigation on Promoted Iron Catalysts for the Synthesis of Ammonia," 3rd ed., Gjellerup, 1968.
3. Kowalczyk, Z., *Catal. Lett.* **37**, 403 (1996).
4. Kowalczyk, Z., Sentek, J., Jodzis, S., Muhler, M., and Hinrichsen, O., *J. Catal.* **169**, 407 (1997).
5. Stoltze, P., *Phys. Scripta.* **36**, 824 (1987).
6. Stoltze, P., and Nørskov, J. K., *Phys. Rev Lett.* **55**, 2502 (1985).
7. Stoltze, P., and Nørskov, J. K., *Surf. Sci. Lett.* **197**, L230 (1988).
8. Stoltze, P., and Nørskov, J. K., *J. Catal.* **110**, 1 (1988).
9. Stoltze, P., and Nørskov, J. K., *Topics in Catal.* **1**, 253 (1994).
10. Bowker, M., Parker, I. B., and Waugh, K. C., *Appl. Catal.* **14**, 101 (1985).
11. Parker, I. B., Waugh, K. C., and Bowker, M., *J. Catal.* **114**, 457 (1988).
12. Bowker, M., Parker, I. B., and Waugh, K. C., *Surf. Sci.* **197**, L223 (1988).
13. Bowker, M., *Catal. Today* **12**, 153 (1992).
14. Fastrup, B., *Topics in Catal.* **1**, 273 (1994).
15. Dumesic, J. A., and Trevino, A. A., *J. Catal.* **116**, 119 (1989).
16. Aparicio, L. M., and Dumesic, J. A., *Topics in Catal.* **1**, 233 (1994).
17. Fastrup, B., and Nielsen, H. N., *Catal. Lett.* **14**, 233 (1992).
18. Rosowski, F., and Muhler, M., *in* "Dynamics of Surfaces and Reaction Kinetics in Heterogeneous Catalysis," p. 111. Elsevier, Amsterdam, 1997.
19. Højlund Nielsen, P. E., *in* "Ammonia, Catalyst and Manufacture" (A. Nielsen, Ed.), p. 191, Springer-Verlag, Berlin/New York, 1995.
20. Ertl, G., Lee, S. B., and Weiss, M., *Surf. Sci.* **114**, 527 (1982).
21. Fastrup, B., *J. Catal.* **150**, 345 (1994).
22. Nielsen, A., *Catal. Rev. Sci. Eng.* **23**, 17 (1981).
23. Ertl., G., Lee, S. B., and Weiss, M., *Surf. Sci.* **111**, L711 (1981).